COMPRESSIVE STRENGTH ANALYSIS OF ADDITIVELY MANUFACTURED ZIRCONIA HONEYCOMB SANDWICH CERAMIC PARTS WITH DIFFERENT CELLULAR STRUCTURES

Betül KAFKASLIOĞLU YILDIZ[1]*, Elif IŞIK[1], Ali Suat YILDIZ[2]

[1]*Sivas University of Science and Technology, Department of Metallurgical and Materials Engineering, 58000, Sivas, Türkiye*
[2]*Sivas University of Science and Technology, Department of Mechanical Engineering, 58000, Sivas, Türkiye*

Abstract: In this study, ZrO_2 honeycomb sandwich structures with different cellular geometry were manufactured by SLA 3D-printing technology to analyze the compressive strength behaviour. After the printing procedure, the samples were sintered at 1450 °C for 2h. Among the samples with different cellular geometry, ZrO_2 parts with circular cells were superior to that of square and triangular honeycomb structures and 1867±320 MPa compressive strength was obtained for this structure. The stress distributions in honeycomb structures were investigated using the COMSOL Multiphysics® for exposing the effect of cellular geometry on compressive strength. While more uniform stress distributions were seen on the inner wall of the circular honeycomb sample, the cellular structure of the square and triangle honeycomb samples mostly displayed compressive stress concentration on the joints of the honeycomb structure. Also, according to Rankine failure criterion, the parts with square cellular geometries were found to be more prone to failure. The highest specific compressive strength was obtained for the ZrO_2 parts with circular cellular geometry. These findings demonstrated that the ZrO_2 honeycomb sandwich structures with circular cellular geometry produced using SLA ceramic 3D-printing technology may be a suitable material to utilize in lightweight structural designs.

Keywords: ZrO_2, SLA, Honeycomb sandwich, Compressive strength

1. Introduction

Advanced ceramics are in demand for a variety of engineering applications because of their superior mechanical and physical qualities (Schwentenwein et al., 2014; Chen et al., 2019). Zirconia (ZrO_2) is one of the most attractive high tech ceramics because of its mechanical characteristics and broad variety of uses such as energy, biomedical, aerospace, mechatronics etc. (Chang et al., 2022; Wang et al., 2023). ZrO_2 ceramics have also high hardness, outstanding wear resistance and thermal stability properties (Manicone et al., 2007; Wang et al., 2023). Nevertheless, complexly shaped ZrO_2 parts are challenging to fabricate due to brittle character, high hardness and wear resistance of the material. Additive manufacturing (AM) offers the potential to manufacture intricately formed ZrO_2 parts. AM, often known as 3D printing technology is utilized to build intricate three-dimensional objects layer by layer using metals, polymers, and ceramics (Buchanan and Gardner, 2019; Zhou et al., 2020; Shen et al., 2021). Since it is very difficult to fabricate ceramic objects with complicated shapes using traditional production methods, ceramic 3D printing technology is one of the most promising and demanding approaches to this problem. Several

techniques, including stereolithography (SLA), selective laser melting/sintering (SLM, SLS), and digital light processing (DLP), are available for 3D printing. Among these technologies, the use of SLA in 3D printing has garnered significant interest for producing ceramics with intricate and complicated architectures because of the highest level of accuracy that ensures industrial quality results from the SLA production process (Lu et al., 2021; Shen et al., 2021; Yu et al., 2023; Wang et al., 2023).

Sandwich structures are becoming increasingly common in lightweight design for high-performance applications, particularly in the automotive, and aerospace industries. Because of its periodic structure and customizable anisotropic qualities, honeycomb offers greater control over features as core of sandwich structures (Haldar et al., 2016; Wang et al., 2019). Honeycomb structures can achieve improved material efficiency if they can be built for particular loading circumstances due to their periodicity and anisotropy. In a wide range of industries, including architectural, automotive, railway, aircraft, satellites, electronic communications, nanofabrication, and medical implants, honeycomb materials have been well-developed and widely employed (Zhang et al., 2015; Qi et al., 2021; Shirvani et al., 2023).

The use of honeycomb ceramic sandwich structures (CSSs), which are often made out of solid ceramic face-sheets and a lightweight ceramic honeycomb core, has gained popularity in recent years. Due to high stiffness and strength to weight ratios and low thermal expansion coefficient, honeycomb CSSs are also being studied as a potential promotional material for example for the next generation of spacecraft thermal protection systems (Srikanth et al., 2017; Hu and Wang, 2021). The utilisation of SLA has emerged as the primary method for producing intricately formed porous ceramics (Chen et al., 2023). This technology has enabled the creation of several porous complex shapes, including micro-lattices, honeycombs, micro-scale trusses (Shen et al., 2021; Xu et al., 2023). In this respect, the investigation of the compressive strength of ZrO_2 sandwich honeycomb structures prepared via SLA printing technology for structural applications, has been the research subject of this study. Because ceramic sophisticated materials and structures are brittle by nature and strength is a key consideration. Compression strength properties were analyzed for lattice ceramic structures prepared by 3D printing in various studies (Fabris et al., 2019; Mamatha et al., 2020; Mei et al., 2021). However, experimental evaluation of compressive strength of ceramic honeycomb structures is very rare (Mamatha et al., 2020). It is important to examine the mechanical behavior and performance of ceramic honeycombs, especially sandwich honeycomb structures, under compressive load and their suitability for structural applications after they are produced with a 3D printer for a functional ceramic material as ZrO_2. Based on this, this paper proposed to prepare various ZrO_2 honeycomb sandwiches with different cellular structures (square, triangle, circle) by SLA technology, and these structures were obtained by pressureless sintering.

2. Materials and Methods

3 mol% Y_2O_3 stabilized ZrO_2 (YSZ) cylinders were printed by a ceramic 3D-printer (C100 Easy Lab, 3DCERAM, France) for mechanical testing using proprietary ceramic-filled photosensitive resin formulation (3DMIX ZR3-E02) on the SLA 3D printer. The size of the cylinders was determined considering ASTM C-1424 standard for compressive strength test in 6.35 mm diameter and 12.1 mm height. The CAD models of the parts prepared for printing are presented in Figure 1. The designed honeycomb cellular structures comprise lower and upper face-sheets (height of each: 0.3 mm) with a honeycomb core (height: 11.5 mm). Details of the hole diameters and cell dimensions of all samples can be seen in Figure 2.a in addition to Figure 1. Both the dimensions of cells and holes and thickness of lower and upper face-sheets were determined considering Kafkaslıoğlu Yıldız et al. (2024) study. The scale factor values given by the supplier were considered to ensure dimensional accuracy after sintering. The printing process operates a 405 nm UV laser to cure the slurry layer-by-layer. The laser power was adjusted to 120 mW, and the layer thickness was set to 50 μm during the printing process at room temperature. First, a metal blade is used to evenly spread the ZrO_2 slurry on the magnetic paper on the working platform. Then, the laser head scans linearly to cure the ceramic slurry in accordance with the cross-sectional shape of the layer that is now in place. The working platform descends to construct another layer after the first layer has formed. Until the entire ZrO_2 component is created, this process is repeated. Fifteen green samples were prepared for each cellular structure. The samples on printing table after the printing process are seen in Figure 2.b.

Following the printing process, the remaining uncured slurry was removed from the green bodies by thoroughly cleaning them with Ceracleaner and compressed air. Debinding is required to remove the organic materials from the green bodies following the 3D printing process. Debinding was carried out in multiple stages up to 615 °C in nitrogen atmosphere using the supplier's thermal cycle. The brown bodies were sintered by heating to 1150 °C at 3.0 °C/min, then proceeding to 1450 °C at 2.0 °C/min by holding 2 h in air in a box furnace (Protherm MOS-B 170/4, Alserteknik, Türkiye).
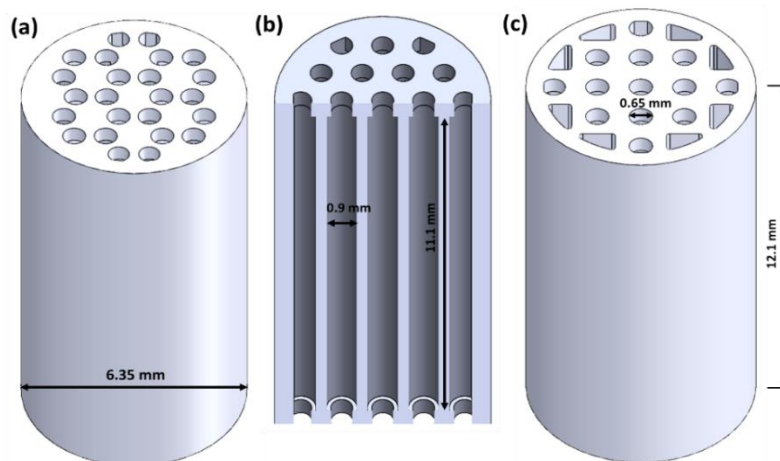
Figure 1. CAD models of the parts before printing process for the samples with a) triangular, b) circular, c) square cellular geometry.
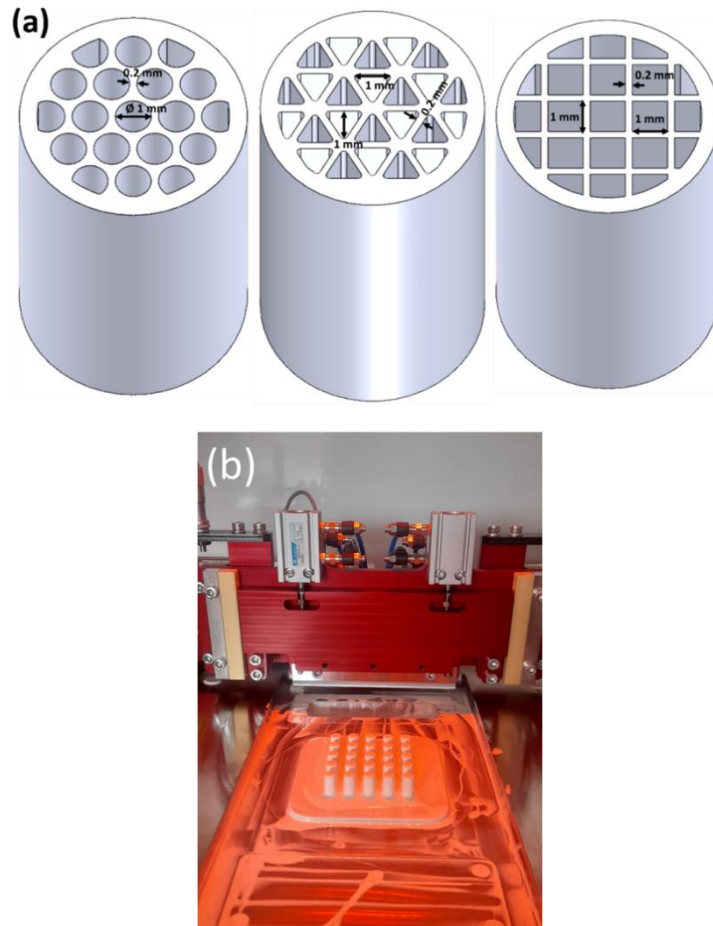
Figure 2. a) Detailed cell dimensions of the parts, b) the samples on printing table after 3D-printing.

From mass and sizes, the bulk density of the sintered ceramic bars was calculated using a volumetric method. The volume values were calculated based on the sample dimensions measured with a caliper. The bulk density to theoretical density ratio of YSZ (6.10 g/cm³) was used to calculate the relative density values. The compressive strength tests of all the ceramic structures were performed by an electronic universal testing machine (Shimadzu AGS-X) equipped with a 50 kN load cell at a loading speed of 0.2 mm/min and the load-displacement curves were recorded until the samples failed at room temperature. To reduce friction, oil (oleic acid) was applied to the surfaces of the samples in contact with the device. Fifteen samples were tested for every cellular structure. The compressive strength of the samples was calculated using the formula given in equation 1 (Mei et al., 2021):

$$\sigma_c = \frac{P}{S} \tag{1}$$

where σ_c, P, and S are the compressive strength, maximum load, and cross-sectional area of a honeycomb, respectively. In addition, the stress distributions created by compression loads were examined using the software COMSOL Multiphysics® in order to explain the strength difference caused by the cellular geometry of the honeycomb structures.

3. Results and Discussion

After the sintering process, the relative densities were 57.0±0.3, 65.6±0.5, and 64.2±0.5 for the honeycomb sandwich samples with square, triangular, and circular cellular geometries, respectively. This difference between the relative density values was related to the difference in the hollow spaces of the samples with different cellular geometry. This was also evident from their average mass. The average mass of the samples were 1.32, 1.52, 1.50 g for square, triangular and circular cellular geometry, respectively. The cross-sections of the samples were also observed on an optical microscope after sintering as given in Figure 3. The samples could be obtained in almost the designed dimensions (both internal and external dimensions) after printing and sintering. Since the shrinkage ratios of the samples were different in X (1.27), Y (1.26), and Z (1.31) axis, there was a difference of 0.1 mm in the designed cell diameters for every geometry and a difference of 0.1 mm in the distance between two cells for the sample with a circular cell geometry.

Figure 4 shows the result of the compressive strength tests for the honeycomb sandwich samples with different cellular structure. As can be seen, the highest average strength was obtained for the honeycomb sandwich structure with circular cellular geometry as 1867±320 MPa. It is well known fact that the advanced ceramics are

inherently brittle materials, therefore mechanical properties like compressive strength can vary considerably. Beside material inhomogeneity such as porosity and the presence of microcracks, the ceramic 3D printing process itself can introduce inconsistencies and small defects can cause considerable variations in compressive strength (Huang et al., 2023). While calculating the compressive strength values, solid cross-sectional areas were taken into account. Examinations and calculations were carried out on the core structure regions (11.5 mm) as the upper and lower face-sheets were very thin (0.3 mm). The solid cross-sectional areas were calculated using an optical microscope image of the samples by Image J. The solid area values were 18.28, 21.64, and 20.17 mm^2 for the samples with square, triangular and circular cellular geometry, respectively. The highest compressive strength was not obtained for the triangular cellular geometry, which had the highest solid cross-sectional area. The difference between the compressive strength values of the samples was mostly related to stress concentrations depending on the cellular geometry.

To better interpret the effect of cellular geometry on compressive strength, the stress distributions in honeycomb structures were investigated using solid mechanics module with a linear elastic material of COMSOL Multiphysics®. The Young's modulus, density, and Poisson ratio of the specimen were set to 188 GPa, 6.10 g/cm^3, and 0.3, respectively. Then the model was meshed using a physics-controlled mesh with a Free Tetrahedral with fine size element. The number of degrees of freedom is changing from 742266 to 2049480. The first principal stress distribution in the 1 mm above the bottom closing surface is shown in the Figure 5. When the analysis results were compared, cellular structure of square and triangle honeycomb sample mostly exhibited compressive stress concentration on the junctions of the honeycomb structure, while more uniform stress distributions were observed on the inner wall of the circular honeycomb sample. This finding was also in agreement with the compressive strength values given in Figure 4.
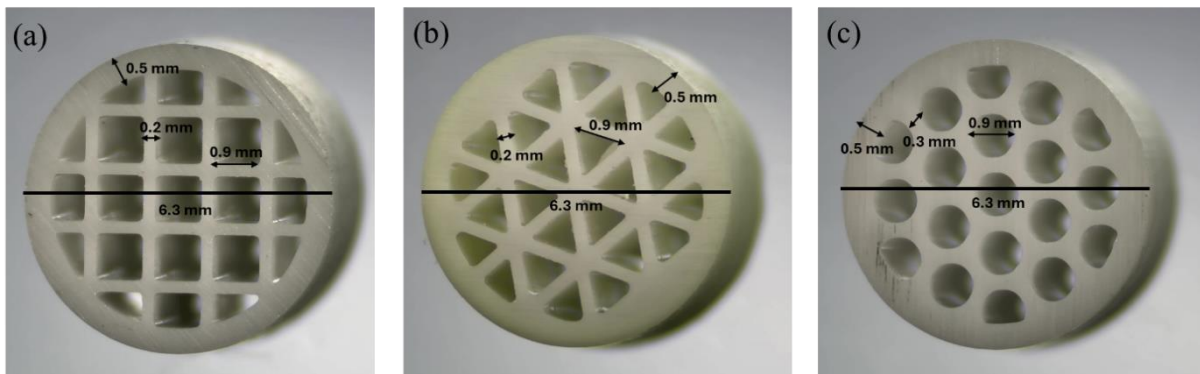
Figure 3. Optical microscope images of the cross-sections of honeycomb samples with a) square, b) triangular, and c) circular cellular geometry.
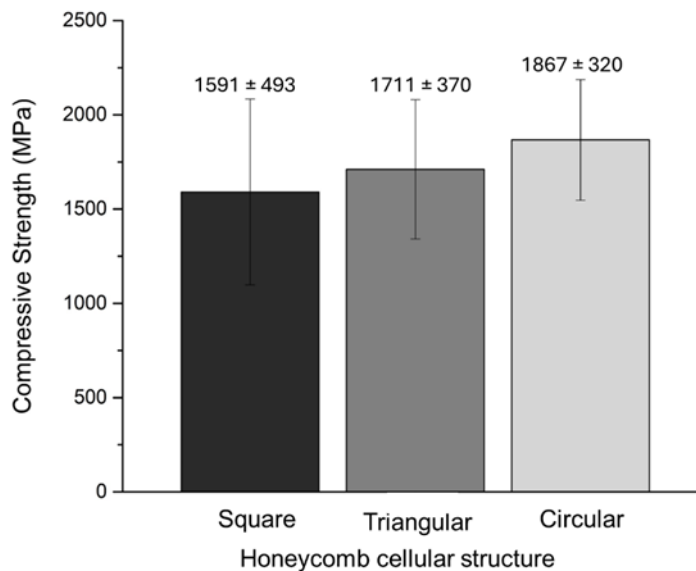
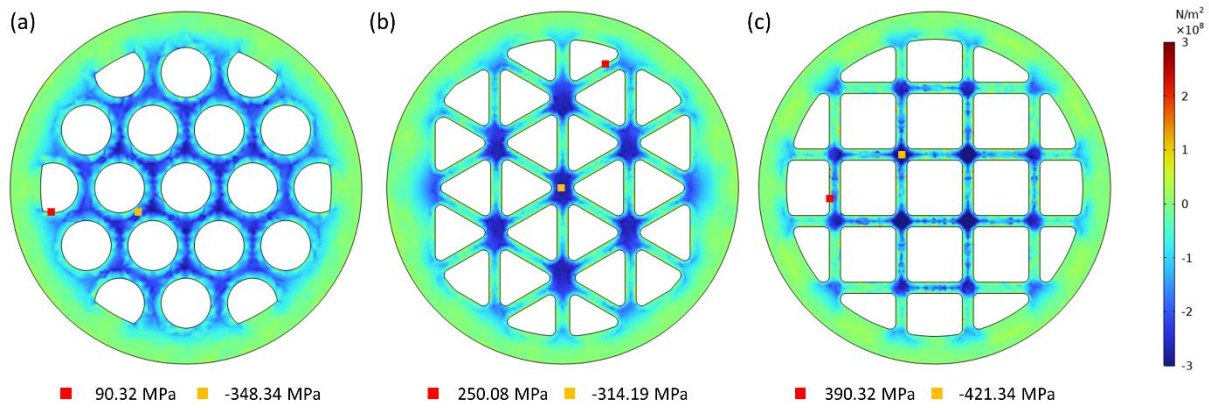**Figure 4.** Compressive strength of the honeycomb sandwich ZrO_2 samples with different cellular structure.

Figure 5. First principal stress state of the samples with a) circular, b) triangular, and c) square cellular structure.
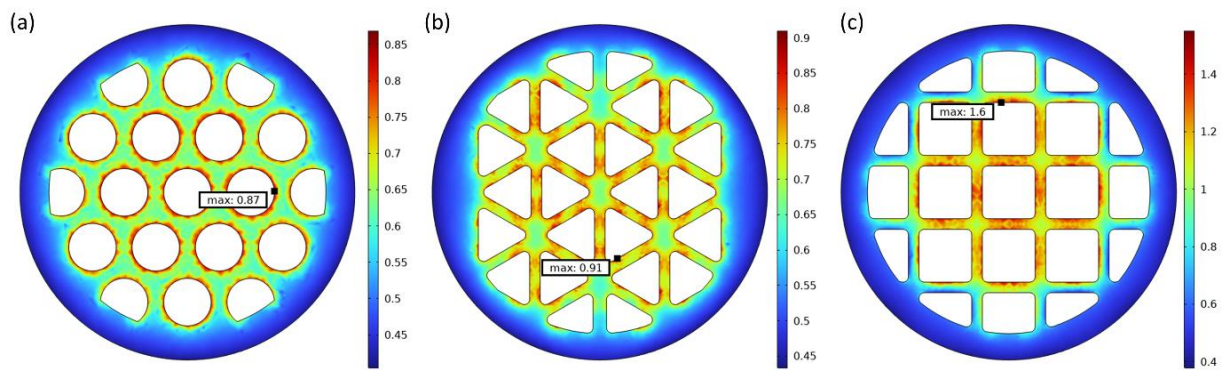

Figure 6. Failure index of honeycomb structures with different cellular geometries.

The compressive strength of the material was defined as 2500 MPa and the geometries were checked for the risk of failure according to the Rankine criterion (maximum normal stress criterion). Here, values greater than 1 on the cross-sectional area can cause crack propagation. Under a force of 29 kN, the Rankine failure index values were calculated for volume average as 0.559, 0.601, and 0.701 for circular, triangular and square cellular geometries, respectively. It can be inferred that the samples with triangle cellular geometry exhibited a 7.5% lower strength than their circular geometry counterparts. This finding was also in agreement with the compressive strength values showed in Figure 5 as 8.35%. Also, the distribution of the Rankine failure criterion across the cross-section were checked for the risk of failure. When the distribution of the Rankine failure criterion across the cross-section of 1 mm below the top surface, where the compressive force was applied, as presented in Figure 6, the parts with square cellular geometries were found to be more prone to failure. The lower strength of the honeycomb structures can be attributed to the stress concentration inner wall for the triangle and square core geometries.

After expressing the strength difference of the samples depending on the cellular geometry, it is necessary to examine the specific strength relationship, which is important for honeycomb sandwich structures (Xue et al., 2022). The material's resistance to compressive loads

in relation to its density is measured by its specific compressive strength. A high specific compressive strength guarantees that honeycomb sandwich ceramics, which are frequently employed in structural applications where weight is a crucial consideration, can support significant loads while maintaining their lightweight nature. Maintaining the structural integrity of parts and structures depends on this attribute. The lightweight nature of ceramic materials for honeycomb sandwich construction is one of its main benefits. Lightweight structures can be built with high specific compressive strength without sacrificing strength or durability. This is especially helpful in the automotive, marine, and aerospace industries as lighter vehicles can result in better load capacity, fuel economy, and performance. The highest specific compressive strength was obtained for the ZrO_2 parts with circular cellular geometry while the other structures were nearly same specific strength level as shown in Figure 7. Ultimately, this study showed that ZrO_2 honeycomb sandwich structure with circular cellular geometry produced using SLA technology is an appropriate choice to use in such materials for lightweight structural designs.
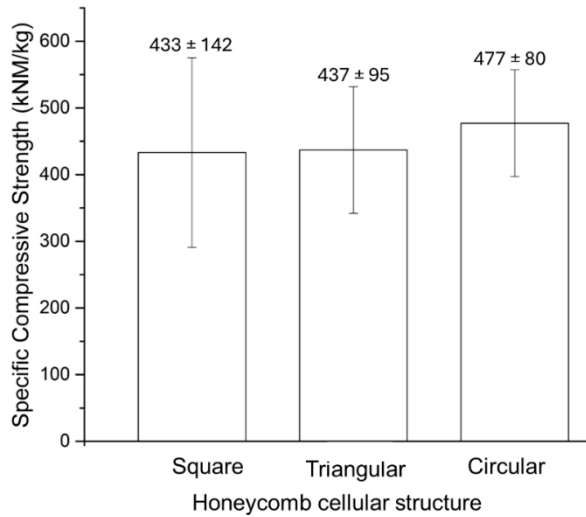
Figure 7. Specific compressive strength values of honeycomb sandwich samples with different cellular geometry.

4. Conclusion

SLA 3D-printing technology was used to prepare ZrO_2 honeycomb sandwich structures with different cellular geometry. The compressive strength of the parts was investigated experimentally and effect of cellular geometry on strength was analyzed by finite element analysis. The highest compressive strength values were attained for the samples with circular cellular geometry as 1867±320 MPa due to stress concentration difference with the other cellular geometries; square and triangular. Also, it was found that square cellular geometries were found to be more prone to failure compared to other structures according to the Rankine failure criterion. When the specific compressive strength examination of the samples was carried out, it was seen that the ZrO_2 honeycomb sandwich samples, which also have circular geometry, was the most suitable design that can be recommended for lightweight structural applications with the highest specific strength.

Conflict of Interest

The authors declared that there is no conflict of interest.

Ethical Consideration

Ethics committee approval was not required for this study because of there was no study on animals or humans.

References

Buchanan C, Gardner L. 2019. Metal 3D printing in construction: A review of methods, research, applications, opportunities and challenges. Eng Struct, 180: 332-348.

Chang J, Zou B, Wang X, Yu Y, Chen Q, Zhang G. 2022. Preparation, characterization and coloring mechanism of 3D printed colorful ZrO2 ceramics parts. Mater Today Commun, 33: 104935.

Chen J, Su R, Zhai X, Wang Y, Gao X, Zhang X, Zhang Y, Zhang Y, Liu S, He R. 2023. Improving the accuracy of stereolithography 3D printed Al2O3 microcomponents by adding photoabsorber: Fundamentals and experiments. JMR&T, 27: 757-766.

Chen Z, Li Z, Li J, Liu C, Lao C, Fu Y, Liu C, Li Y, Wang P, He Y. 2019. 3D printing of ceramics: a review. J Eur Ceram Soc, 39: 661-687.

Fabris D, Mesquita-Guimarães J, Pinto P, Souza JCM, Fredel MC, Silvab FS, Henriques B. 2019. Mechanical properties of zirconia periodic open cellular structures, Ceram Int, 45: 15799-15806.

Haldar AK, Zhou J, Guan Z. 2016. Energy absorbing characteristics of the composite contoured-core sandwich

panels. Mater Today Commun, (8): 156-164.

Hu JS, Wang BL. 2021. Crack growth behavior and thermal shock resistance of ceramic sandwich structures with an auxetic honeycomb core. Compos Struct, 260: 113256.

Huang Z, Liu LY, Yuan J, Guo H, Wang H, Ye P, Du Z, Zhao Y, Zhang H, Gan CL. 2023. Stereolithography 3D printing of Si3N4 cellular ceramics with ultrahigh strength by using highly viscous paste. Ceram Int, 49: 6984-6995.

Kafkaslıoğlu Yıldız B, Yıldız AS, Kul M, Tür YK, Işık E, Duran C, Yılmaz H. 2024. Mechanical properties of 3D-printed Al2O3 honeycomb sandwich structures prepared using the SLA method with different core geometries. Ceram Int, 50: 2901-2908.

Lu J, Dong P, Zhao Y, Zhao Y, Zeng Y. 2021. 3D printing of TPMS structural ZnO ceramics with good mechanical properties. Ceram Int, 47: 12897-12905.

Mamatha S, Biswas P, Das D, Johnson R. 2020. 3D printing of cordierite honeycomb structures and evaluation of compressive strength under quasi-static condition. Int J Appl Ceram Technol, 17: 211-216.

Manicone PF, Iommetti PR, Raffaelli L. 2007. An overview of zirconia ceramics: basic properties and clinical applications. J Dent, 35(11): 819-826.

Mei H, Tan Y, Huang W, Chang P, Fan Y, Cheng L. 2021. Structure design influencing the mechanical performance of 3D printing porous ceramics. Ceram Int, 47: 8389-8397.

Qi C, Jiang F, Yang S. 2021. Advanced honeycomb designs for improving mechanical properties:A review, Compos B Eng, 227: 109393.

Schwentenwein M, Schneider P, Homa J. 2014. Lithography-based ceramic manufacturing: a novel technique for additive manufacturing of high-performance ceramics. Adv Sci Technol, 88: 60-64.

Shen M, Qin W, Xing B, Zhao W, Gao S, Sun Y, Jiao T, Zhao Z. 2021. Mechanical properties of 3D printed ceramic cellular materials with triply periodic minimal surface architectures. J Eur Ceram Soc, 41: 1481-1489.

Shirvani SMN, Gholami M, Afrasiab H, Talookolaei RAJ. 2023. Optimal design of a composite sandwich panel with a hexagonal honeycomb core for aerospace applications. Iranian J Sci Technol Trans Mech Eng, 47: 557-568.

Srikanth O, Khivsara SD, Aswathi R, Madhusoodana CD, Das RN, Dutta VSP. 2017. Numerical and experimental evaluation of ceramic honeycombs for thermal energy storage. Trans Ind Ceram Soc, 76(2): 102-107.

Wang L, Yao L, Tang W, Dou R. 2023. Effect of Fe2O3 doping on color and mechanical properties of dental 3Y-TZP ceramics fabricated by stereolithography-based additive manufacturing. Ceram Int, 49: 12105-12115.

Wang Z, Lia Z, Xiong W. 2019. Numerical study on three-point bending behavior of honeycomb sandwich with ceramic tile, Compos B Eng, 167: 63-70.

Xu H, Li S, Liu R, Bao C, Mu M, Wang K. 2023. Fabrication of alumina ceramics with high flexural strength using stereolithography. IJAMT, 128: 2983-2994.

Xue D, He L, Tan S, Li Y, Xue P, Yang X. 2022. Study on compression characteristics of honeycomb sandwich structure with multistage carbon fiber reinforced composites. Polym Compos, 43: 6252-6264.

Yu X, Wang Z, Wang Y, Yu Z, Zhao Y, Zhao J. 2023. Optimization, formation, and evolution of the photoinduced curing gradients and in-situ lamellar gaps in additive manufacturing of ZrO2 ceramics: From curing to sintering behaviors. J Eur Ceram Soc, 43: 6279-6295.

Zhang Q, Yang X, Li P, Huang G, Feng S, Shen C, Han B, Zhang X, Jin F, Xu F, Lu TJ. 2015. Bioinspired engineering of honeycomb structure – Using nature to inspire human innovation. Prog Mater Sci, 74: 332-400.

Zhou LY, Fu J, He Y. 2020. A review of 3D printing technologies for soft polymer materials. Adv Funct Mater, 30(28): 2000187.